Microbial Pathogenesis 166 (2022) 105553

Contents lists available at ScienceDirect

Microbial Pathogenesis

journal homepage: www.elsevier.com/locate/micpath

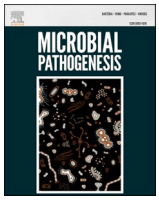

The circulating plasma metabolome of *Neoparamoeba perurans*-infected Atlantic salmon (*Salmo salar*)

Carlo C. Lazado [a,*], Mette W. Breiland [b], Francisco Furtado [a,c], Erik Burgerhout [b], David Strand [d]

[a] Nofima, Norwegian Institute of Food Fisheries and Aquaculture Research, 1433, Ås, Norway
[b] Nofima, Norwegian Institute of Food, Fisheries and Aquaculture Research, 9019, Tromsø, Norway
[c] CIISA, Faculty of Veterinary Medicine, University of Lisbon, 1300-477, Lisbon, Portugal
[d] Norwegian Veterinary Institute, 1433, Ås, Norway

ARTICLE INFO

Keywords:
Amoebic gill disease
Aquaculture
Gill health
Metabolomics
Mucosal immunity

ABSTRACT

Metabolomics can provide insights into the dynamic small-molecule fluctuations occurring in response to infection and has become a valuable tool in studying the pathophysiology of diseases in recent years. However, its application in fish disease research is limited. Here, we report the circulating plasma metabolome of Atlantic salmon (*Salmo salar*) experimentally infected with *Neoparamoeba perurans*—the causative agent of amoebic gill disease (AGD). Plasma samples were collected from fish with varying degrees of infection inferred from an external gross morphological score of gill pathology (i.e., gill score [GS] 1 – GS3), where a higher GS indicates advanced infection stage. Uninfected fish (GS0) served as the control. Typical pathologies associated with AGD infection, such as hyperplastic lesions and lamellar fusion, were evident in infected gill samples. Plasma metabolites were identified by ultra-performance liquid chromatography coupled with a high-resolution quadrupole-orbitrap mass spectrometer. Identification of compounds were performed at four levels of certainty, where level 1 provided the most accurate compound identity. A total of 900 compounds were detected in the samples of which 143 were annotated at level 3, 68 on level 2b, 74 on level 2a, and 66 on level 1. Versus GS0, GS1 showed the highest number of significantly affected metabolites (104), which decreased with a higher GS. Adrenaline and adenosine were the two Level 1 compounds significantly affected by AGD regardless of GS, with the former increasing and the latter decreasing in infected fish. Hippuric acid significantly increased in GS1 and GS2, while the tryptophan metabolite indole-3-lactic acid decreased in response to the initial stage of infection but returned to basal levels at a higher GS. There were ten significantly affected metabolic pathways: Eight of which were significantly downregulated while two were downregulated in GS1 relative to GS0. The super-pathway of purine nucleotide salvage was enriched both within the upregulated metabolites in GS1vsGS0 and the down-regulated metabolites in GS3vsGS1. This is the first report on the circulating plasma metabolome of AGD infected salmon, and the results show that low infection levels resulted in a more dramatic metabolomic dysregulation than advanced infection stages. The metabolites identified are potential biological markers for the systemic physiological impact of AGD.

1. Introduction

Parasitic infestations have severe economic, animal welfare, and ecological impacts on Atlantic salmon (*Salmo salar*) aquaculture. Although sea lice (*Lepeophtheirus salmonis* and members of the *Caligus* genus) remain the major parasitic issue, other parasitic infestations pose serious concerns in salmon farming. Amoebic gill disease (AGD) is a proliferative gill condition primarily affecting the sea cage phase of salmon. It was first described in Tasmania, Australia in 1986, and since then, cases have been documented in the United States, Chile, Ireland, Spain, France, Japan, and Norway [1]. The causative agent, *Neoparamoeba perurans,* is a free-living and opportunistically parasitic amoeba species that attach to the gill lamellae [2]. The severity of AGD in the farms is assessed through histopathological and gill gross evaluations. Infected fish exhibit epithelial multifocal gill hyperplasia, hypertrophy, oedema, and interlamellar vesicle formation [3]. These can be grossly detected by increased mucus production and formation of white mucoid spots and plaques on the gill surface [4]. Behavioural

* Corresponding author.
E-mail address: carlo.lazado@nofima.no (C.C. Lazado).

https://doi.org/10.1016/j.micpath.2022.105553
Received 3 September 2021; Received in revised form 19 April 2022; Accepted 20 April 2022
Available online 25 April 2022

manifestations of AGD include lethargy, anorexia, congregation at the water surface, and increased ventilation rate [5] leading to respiratory distress that can result in mortality between 50 and 80% if left untreated [1,6]. On-farm assessment of AGD is often performed through a systematic scoring of the white mucoid patches and gross lesions on the gills where infestation severity is rated from 0 to 5 [7]. Gill score is a gross measure of the degree of the host response to the presence of *N. perurans,* and the degree of lesion development is known to be in direct proportion to the parasite load and severity of infection [8].

The mucosal pathophysiology of AGD has been elucidated by transcriptomics, proteomics, and targeted biochemical analyses in the gills and mucus. Through microarray analysis, Young and colleagues reported a coordinated down-regulation of the genes involved in the major histocompatibility complex class I (MHC I) pathway in addition to the downregulation of cytokines, particularly interferons, in AGD-affected gills [9]. Upregulation of *mucin 5* and Th2 cytokines (*il4/13a* and *il4/13b2*) were observed in experimental and natural *N. perurans* infections supporting the hallmark responses of salmon to AGD, which include increased hyperplasia and mucus production [10]. It has been further demonstrated that gill transcriptomic responses, particularly the molecular regulators of inflammation (i.e. cytokines) and the different immune cell markers (i.e. antigen presenting cells, B cells and T cells), are highly influenced by regional differences of the lesions [11]. The protein–protein interaction networks generated from gill mucus proteomics revealed that affected proteins formed part of cell to cell signalling and inflammation pathways [12]. Profiling of some key immune markers in the gill mucus of AGD-affected fish showed that IgM levels and the activities of peroxidases, lysozymes, esterases, and proteases, decreased in fish with high disease severity; nonetheless, a sequential recovery was observed after treatment [13]. A similar tendency of immune-suppression associated with AGD was identified in the gills proteomes especially during the initial phase of infection, where inhibition of protein expression with immune signalling, phagocytosis, and T-cell proliferation was documented [14]. A recently published novel model for host-parasite interaction during AGD pathogenesis integrated host and parasite functional response profiles to reveal how the different players for invasion of host, evasion of host defence mechanisms and formation of the mucoid lesion are orchestrated during infection [15].

Despite the advances made in understanding the molecules and processes involved in the mucosal responses of salmon to *N. perurans*, the systemic physiological impacts of AGD infection remains barely understood. Nonetheless, some available studies offered a fragmentary insight into the systemic host response. While, a panel of selected humoral immune parameters was found to be unaffected in serum relative to the gill mucus of AGD-affected salmon [13], a large scale serum proteomic profiling revealed an increase in the expression of immune-related molecules at the early phase of infection followed by a strong inhibition at later stages [14]. Studying the systemic responses of salmon to *N. perurans* will be pivotal to our understanding of the extent of the impact of the parasitic infection and will facilitate the identification of new markers of disease status.

Metabolomics has become a powerful tool in physiological studies in aquaculture, although its application in understanding the onset and development of a disease is limited [16]. In humans, the identification of metabolic biomarkers in diseased individuals has novel potential advantageous features such as more accurate diagnosis, dynamic disease evaluation, non-invasive sampling, or personalised treatment assessment [17]. There has been an increasing regard to metabolomics in salmonid research, where it is widely applied in ecotoxicological and nutritional studies [18]. Its application to understand host-pathogen interaction is still limited though its potential to resolve physiological alterations during host-pathogen interaction is immense. Here, we applied large scale metabolomics in the plasma of salmon exhibiting different AGD infection levels inferred by the gross gill pathology. The profiled circulating metabolomes provide insight into the panel of metabolites altered by parasitic infestation and their role in the adaptive physiological response of salmon to AGD.

2. Materials and methods

2.1. Ethical use of animal for research

The specimens used here were collected from an associated infection trial (Norwegian Food Safety Authority FOTS ID 20/23121) performed at Aquaculture Research Station (Tromsø, Norway). This strategy supports the 3Rs (reduce, replace, refine) in aquaculture research by collecting samples from another trial thus reducing the number of fish used for research.

2.2. Neoparamoeba perurans

The isolate of *Neoparamoeba perurans* used in the trial was retrieved from a natural outbreak in 2019 by the Norwegian Veterinary Institute (facilitated through Sigurd Hytterød). A polyclonal culture (less than 1 year old) was sent to the Fish Health Department of Nofima AS in Tromsø, Norway where its pathogenicity and virulence were established. Thereafter, an infection model was developed for this isolate in another project (Basis Funding-Norwegian Research Council, *AGD-modell*), which was applied in this trial. In this infection model, fish infected with the parasite developed GS 0.5–1 after 8–10 days, GS 1–2 after 14–16 days, and GS 2–3 around 3 weeks. The double gill scoring system developed by Fomas - Fiskehelse og Miljø AS is a modified version of the widely known Taylor system [7] and was used to evaluate the severity of AGD infection. The isolate was routinely cultured in Malt Yeast Broth (with filtered seawater, 35 ppt) at 15 °C.

2.3. Description of the infection trial

Smolts produced at HiT with a starting weight of 83 ± 7.8 g (n = 720) were evenly stocked in two 1000-L octagonal tanks in a flow-through. The fish had been acclimated to seawater for at least 2 weeks before they were transferred to the experimental units. One tank served as the uninfected control group (**Tank C**), and the other tank was used for the infection trial (**Tank I**). In this study, we were only interested in comparing the infected and uninfected fish and considered the individual fish as a biological replicate. Fish were allowed to acclimatise experimental conditions for a week in the before they were exposed to the parasite under the following parameters: water flow rate set at 6–7 L min^{-1}, salinity at 35‰, temperature at 14.0 ± 0.5 °C, dissolved oxygen >90% saturation, photoperiod set at 24 L:0 D, and a continuous feeding regime (Nutra Olympic 3 mm, Skretting, Averøy, Norway). Experimental infection (Tank I) was performed by closing the water flow in the tank, and the fish were exposed to *N. perurans* at an exposure dose of 1500 amoeba/L of water for 1 h. Oxygen was supplied during the experimental infection to maintain a DO >90% saturation and facilitate continuous mixing. After the challenge period, water was flushed and replaced, and the system was operated following the conditions during acclimation. The control-uninfected group (Tank C) was exposed to the same manipulation except no parasite was added. The production protocol employed during the acclimation period was similarly followed during the disease development period.

After three weeks, a group of fish were humanely euthanised with an overdose of benzocaine (Benzoak vet, 200 mg/ml, EuroPharma, Norway), and the gills were scored by an experienced researcher according to the method described above. Five fish were chosen per each GS group (e.g., 1, 2, and 3) and control group, and blood was extracted from the caudal vessels using a heparinised vacutainer (BD Vacutainer™, Fisher Scientific UK Ltd, UK). Plasma was obtained by centrifugation for 10 min at 5000 rpm maintained at 4 °C, and thereafter stored at −70 °C until analysis. Gill swabs (Sarstedt, Germany) were taken from the left side of the gills and stored in ATL buffer (Qiagen, Hilden, Germany) for subsequent detection of the parasite by qPCR. The second gill arch from the

right side was collected and stored in neutral buffered formalin (BiopSafe ApS, Hellerup, Denmark) for consequent histological processing. To reisolate the amoeba, gills from randomly selected fish were excised and sent to the laboratory for isolation and re-culture of the parasite.

2.4. Detection of the parasite in the gill swabs by qPCR

DNA was extracted from the gill swabs using the DNeasy blood and tissue kit (Qiagen). A *N. perurans* specific qPCR assay (David A. Strand, unpublished), with forward primer 5′-GTT CTT TCG GGA GCT GGG AG-3′, reverse primer 5′- CAT GAT TCA CCA TAT GTT AAA TTT CC-3′ and probe 5′-FAM/CTC CGA AAA/ZEN/GAA TGG CAT TGG CTT TTG A/3IABkFQ-3′, was used to analyse the extracted DNA for the presence of *N. perurans*. The samples were analysed on the CFX96 Touch System (Biorad, CA, USA) with 25 μl reactions consisting of 12.5 μl TaqPath qPCR Mastermix, 500 nM of each primer and 250 nM of probe, PCR grade water and 5 μl DNA sample. The following qPCR cycling condition were used: an initial denaturation at 95 °C for 20 s, followed by 50 cycles of denaturation at 95 °C for 3 s and annealing at 60 °C for 30 s. The specificity of the designed assay was analysed *in silico* against closely related organisms by performing a BLAST search at National Center for Biotechnology Information database. The assay was further tested *in vitro* against several in-house (Norwegian Veterinary Institute) *N. perurans* strains and against the closely related organisms N. pemaquidensis, N. branchiphila and N. aestuarina. All of the *N. perurans* strains were amplified with the assay, while *N. pemaquidensis*, *N. branchiphila* and *N. aestuarina* did not amplify. A 10-fold standard dilution using synthesized dsDNA (gBlocks™ gene fragment, Integrated DNA Technologies, Iowa, USA) of the qPCR target region with known DNA concentration was included in each qPCR run in order to estimate the DNA copies per reaction.

2.5. Histology

The formalin-preserved gills were embedded in paraffin following a series of ethanol dehydration, xylene clearing, and paraffin infiltration in a benchtop histoprocessor (Leica TP1020, Germany). Paraffin-embedded tissues were cut into 5-μm-thick sections (Leica RM2165, Germany) and stained with haematoxylin-eosin and digitised using a slide scanner (Aperio CS2, USA).

2.6. Plasma metabolomics

Plasma samples were sent to MS-Omics ApS (Vedbæk, Denmark) for metabolite profiling. The analysis was conducted using a Thermo Scientific Vanquish LC coupled to Thermo Q Exactive HF MS. An electrospray ionisation interface was used as an ionisation source and analysis was performed in negative and positive ionisation modes. An ultra-performance liquid chromatography-tandem mass spectrometry (UPLC-MS/MS) was used with a slightly modified protocol first described by Doneanu et al. [19], which had been applied earlier to salmon plasma samples [20]. Peak areas were extracted using Compound Discoverer 3.1 (Thermo Scientific). Identification of compounds were performed at four levels: **Level 1** offered identification by retention times (compared against in-house authentic standards), accurate mass (with an accepted deviation of 3 ppm), and MS/MS spectra. **Level 2a** used identification by retention times (compared against in-house authentic standards) and accurate mass (with an accepted deviation of 3 ppm). **Level 2b** used identification by accurate mass (with an accepted deviation of 3 ppm) and MS/MS spectra. **Level 3** used identification via accurate mass alone (with an accepted deviation of 3 ppm). For unidentified compounds, the elemental composition was determined if there was a good match between the accurate mass obtained and the isotope pattern.

2.7. Data handling and statistics

Metabolomic data (also referred to as samples in this section) are scored (outliers identified) based on objective scoring methods: commonly used scoring methods are Hoeffding's D-statistic, mean Pearson correlation with other samples, sum of Euclidean distance to other samples, and the Kolmogorov-Smirnov test statistic. Samples were sometimes "blacklisted" (manually failed) or "whitelisted" (manually passed despite failing automatic checks) based on detailed manual inspection and consideration of the experimental design. A sample was classified as an outlier if it failed two or more of these objective parameters. Normalised data provided the input for statistical hypothesis testing in which metabolites that were significantly different between sample groups were identified. Statistical comparisons were performed using linear modelling as implemented in the Bioconductor package limma.

Significance values (p-values) were adjusted for multiple testing, by controlling the false discovery rate. For each comparison (e.g., GS0*vs*GS1), a positive log2 (fold change) indicates up-regulation in GS1 relative to GS0. Significant metabolites (defined using $P < 0.05$) from each comparison were analysed for enrichment of MetaCyc pathway membership (https://metacyc.org/) using a hypergeometric test. Enrichment ($P < 0.05$) was assessed for up-, down-, and bidirectional-regulated metabolites separately.

3. Results and discussion

Alterations in endogenous and environmental factors profoundly impact the organism's metabolome, which acts as an essential chemical bridge connecting the environment with the different levels of a biological system [21]. In particular, infection changes the physiological state of an organism [22] and these modifications are reflected in the identity and nature of metabolites involved in the host responses [23]. Although some studies have shed some insights into these interactions in fish [16,24], the systemic metabolomic consequences of parasitic infestation have been barely explored. To the best of our knowledge, this study is the first to report the plasma metabolome of AGD-affected salmon and one of the few studies in farmed fish that has applied high-throughput metabolomics to unravel host-parasite interactions. We found that AGD altered the circulating metabolome of salmon, and that the changes were more pronounced in fish exhibiting the lowest infection level than in the groups with severely compromised gill status.

The samples were collected at the same time point post-infection; therefore the confounding effect of age [16] has been minimised and the changes observed were predominantly attributed to the disease state. The amoebae were detected by qPCR in all gill swab samples from infected fish, and its absence in the control, uninfected group was likewise verified. In addition, the parasite was re-isolated from the gills of the infected fish and managed to be re-cultured under laboratory conditions. This confirms that the biological samples used in this analysis represents both AGD-free and AGD-affected fish. Further, histopathology evaluation of infected gill samples indicated epithelial hyperplasia and microscopic lesions consistent with AGD (i.e., multifocal hyperplasia and fusion of the lamellar epithelium (Fig. 1), where attached amoebae were observed [25]. Although cases of lifting and lamellar clubbing were also detected in both uninfected and AGD-affected fish, no considerable difference was detected between the groups. The frequency of occurrence is similar to previously reported healthy, AGD-free salmon smolts [20,26]. These changes may likely be non-specific environmental responses and not primarily associated with the disease.

Traditional AGD research focuses mainly on histopathological alterations and molecular response profiling through gene and protein expression in the gills, and recent developments have made significant contributions to unravel the systemic physiological alterations associated with the disease [10,12,13]. AGD has systemic metabolic consequences, and these have been documented by traditional metabolic

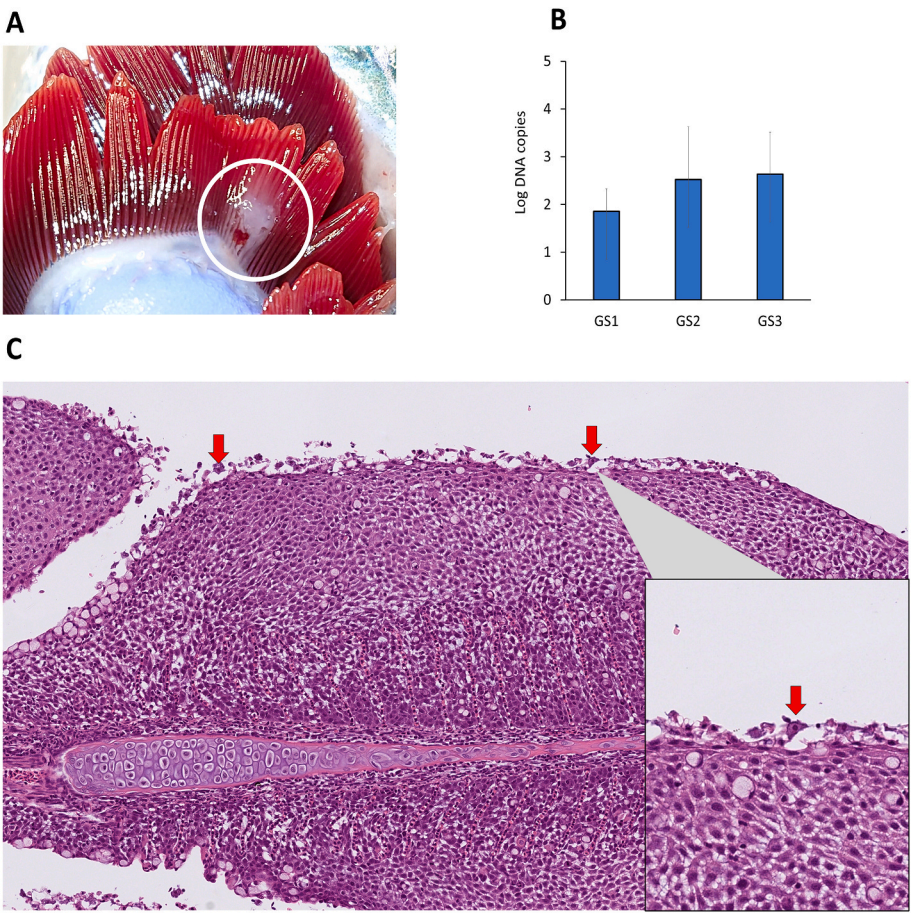

Fig. 1. Gross and microscopic pathologies of AGD-affected salmon. **(A)** Macroscopic AGD lesions in experimentally infected fish showing the typical mucoid patches from the base to the mid-section of the filaments (inside the white circle). **(B)** qPCR detection of *N. perurans*. Log DNA copies are provided. **C)** The gills of AGD-affected fish showing the classical pathologies for AGD including multifocal hyperplasia and fusion of lamellar epithelium, where amoeboid bodies are likewise observed (inset).

assays including respirometry [27] or targeted plasma biochemical analyses, such as quantification of the levels of glucose, lactate, and cortisol [28]. These analytical tools have provided insights into how varying degrees of AGD infection resulted in physiological dysregulation, however, they only slightly captured the extent of systemic changes in infected fish. Metabolomics allowed high-throughput analysis of several hundreds of metabolites associated with different biological pathways, thereby offering a promising tool to understand the overall disease state. Here we showed that AGD altered the plasma metabolome of salmon (Fig. 2) supporting earlier evidence from targeted analysis [13] that the gill parasitic infection triggers not only a local response but also results in systemic physiological dysregulation. Using plasma as a biological matrix for this analysis provides an appropriate snapshot of the disease state, because the analysis of biofluids or tissues from infected hosts represents the most accurate methodology to describe the metabolic changes associated with disease [21]. Future studies must also account tissue-specific metabolomic response, given that the disease state of the gills have profound impact on distant organs such as head kidney and spleen [15]. This will facilitate the understanding of the metabolomic regulators of different organs with known key involvement in orchestrating host responses to AGD, thereby, establishing a global snapshot of inter-tissue communication during infection.

We have identified 900 compounds in the samples (Supplementary File 1). Of these, 143 compounds were annotated on level 3, 68 on level 2b, 74 on level 2a, and 66 on level 1. Only these compounds were included for further analysis, and the unannotated compounds were provided in the Supplementary File 1 for future reference.

The effects of AGD infection level (assessed by gross gill score) on the plasma metabolome were more pronounced when the level of infection was low (Fig. 2). This was clearly shown with the decreasing number of differentially affected metabolites (DAM) relative to GS0 (uninfected fish) in fish with higher GS (Fig. 2A–C). There were 104, 39, and 20 DAM in GS1, GS2, and GS3, respectively (Fig. 2A–C). Despite this clear tendency of decreasing number of DAM at higher GS, the distribution of upregulated and downregulated metabolites remained consistent across different comparisons with no clear distinction suggesting that the pattern of dysregulation is not dependent on GS at least within the range used here. It would be interesting to explore in the future whether such a profile is still evident at GS $>$ 3, where the gills are already severely compromised. Likewise, the correlation of the metabolomic responses between laboratory and natural infections is an area that should be explored further to expand our knowledge on how metabolome is altered during AGD.

We further compared the DAM amongst GS within infected fish (Fig. 2D–F). The profiles further suggested that fish with GS1 demonstrated marked metabolomic dysregulation compared with GS2 (Fig. 2D) and GS3 (Fig. 2F). The lowest number of identified DAM was between GS2 and GS3 (Fig. 2E) indicating that metabolomic changes between moderate and severe cases of infection were minimal. The fish were challenged at the same time, and the period of disease development is similar for all infected fish used in the analysis. Therefore, the plasma metabolome captured the disease state and offered insights into how some fish were more susceptible while others could ward off infection in the same environment and with a similar infection history. The pronounced alterations in the plasma metabolome with lower GS may be related to the continuous active physiological adaptations to fight off the infection and would not allow it to develop further. As the severity of infection progressed, the fish became less able to mobilise the required metabolites to combat the pressure of infection, which could indicate an impairment of adaptive physiological response. It was earlier reported that immunity is impaired when the severity of AGD infection progressed as demonstrated by gene expression studies [13,29]. This

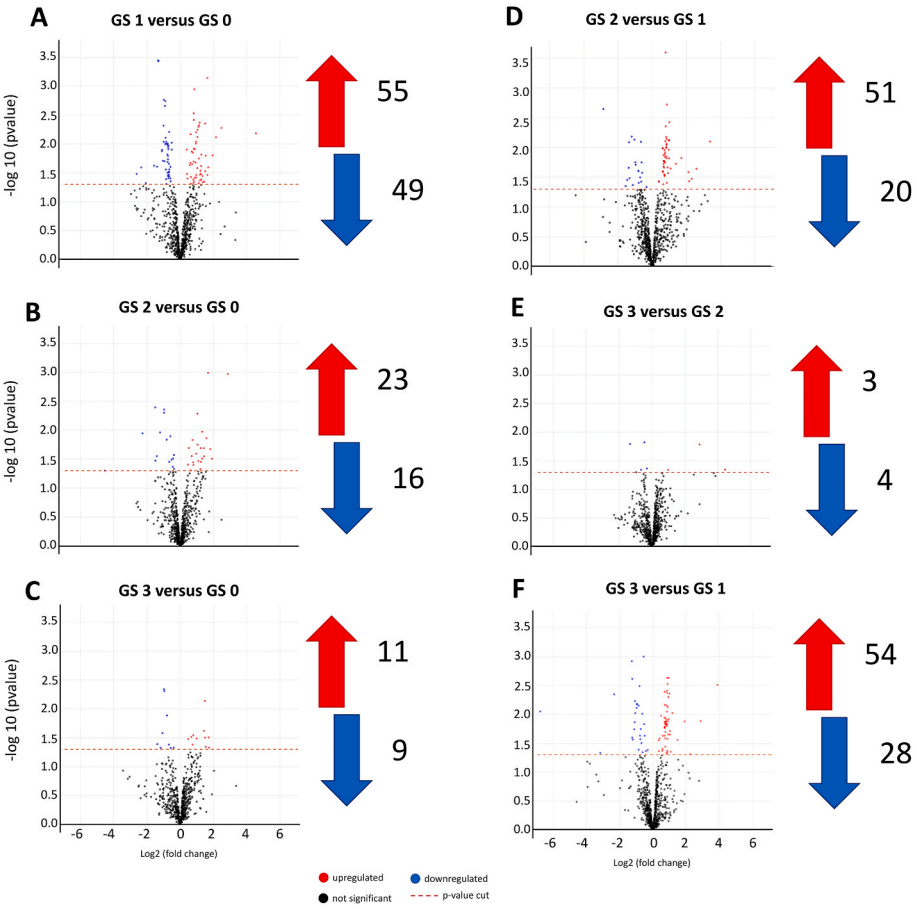

Fig. 2. Volcano plots showing significance (as -log10 transformed p-values) against magnitude (log2(fold change)) of differentially affected metabolites. Metabolites identified as having different levels between samples are represented as red (up-regulated) or blue (down-regulated) dots/arrows. Numbers appearing beside the arrow indicates the actual number of metabolites in that specific group. To improve performance when there are tens or hundreds of metabolites, the non-significant metabolites displayed in black are a representative subsample of the entire dataset. For this set of comparisons, significantly differentially expressed metabolites were defined as those with a p-value < 0.05 represented by the horizontal orange line. The full list of metabolites per comparison is provided in Supplementary File 2.

similar tendency of physiological response is reflected in the plasma metabolome. Metabolites can shape the function of immune cells and thus playing an important function in the outcome of immune responses [30]. The metabolomic profile in the present study and the immune response identified earlier for AGD establish a potential link between metabolites and immune regulators in resolving the host response to AGD. These profiles likewise reveal that the application of metabolomics for AGD is perhaps more appropriate during the early stage of infection because we observed striking changes on this infection level.

To investigate the overlap between selected metabolites from the multiple contrasts performed (Fig. 2), we counted the number of overlapping DAM (defined using p-value<0.05) between all pairwise combinations of the comparisons performed, and the amount of overlap is represented in a heatmap (Fig. 3A). Most of the significant overlap was found when contrast was made against the DAM of GS1*vs*GS0. In particular, the highest number of overlaps were found in the following comparisons: GS1*vs*GS0 **versus** GS3*vs*GS1, GS1*vs*GS0 **versus** GS2*vs*GS1, and GS2*vs*GS1 **versus** GS3*vs*GS1. Notably, the fold changes of the metabolites from the contrasts GS1*vs*GS0 **versus** GS3*vs*GS1 (Fig. 3B) and GS1*vs*GS0 **versus** GS2*vs*GS1 (Fig. 3C) were significantly negatively correlated. This may indicate that some changes observed in the low infection level are subsequently reversed as the infection progresses/regresses; or normal physiological functions may be inhibited in advanced infection stage.

Regarding the DAM, adrenaline and adenosine were the two Level 1 DAM found in all AGD-affected fish (GS1-3) suggesting the important role of these molecules in the systemic responses of salmon to AGD (Fig. 4). Notably, adrenaline showed a larger than 4-fold increase in abundance when comparing infected (GS1 to GS3) to uninfected (GS0) fish (Fig. 4A). A similar statistically significant increase in adrenaline was observed upon comparing individual infected groups to uninfected samples. Adrenaline is a steroid hormone that participates in the stress response of fish and is produced from the hydroxylation of phenylalanine to tyrosine [31]. One of the adaptive physiological responses of salmon to AGD is the mobilisation of stress response such as the induction of plasma cortisol that is linked to the mediation of inflammation during infection [32,33]. On the other hand, immunosuppression has been documented in AGD-affected salmon [10,13,28]. Neuroendocrine hormones have important role in immunity where bidirectional communication between the endocrine and immune systems via hormones and cytokines have been established [34]. Hence, it could be possible that the increased plasma adrenaline level likely mediated immunosuppression because it has been shown to have an immunosuppressive role in fish [35]. In humans, adrenaline has been identified to regulate T cells and the regulatory function seems to indicate that it directly inhibit the T cells but not for their precursors [36]. Though such a relationship remains to be fully elucidated in fish, we speculate that the pronounced changes in adrenaline in the study present a potential cellular trafficking mechanism of T cells during AGD infection. The previous study that identified T-cells increase within the AGD-affected gills, where $CD8^+$ cells and not $CD4^+$ T-cells were prominent [11], lends support to this interplay and hence, an area for further exploration.

Adenosine was 1.6-fold less abundant in infected samples than healthy samples (Fig. 4B). This trend was observed in GS1 to GS3 when compared to GS0. Adenosine is a naturally occurring nucleoside present in various cell types. It is an essential molecule for energy production and utilisation, and it exerts profound immune regulatory functions in many organisms [37]. In particular, it has anti-inflammatory properties [38]; therefore, its downregulation in infected fish suggest interference of its putative role in inflammation, perhaps in the recruitment of immune cells. Earlier, AGD was shown to have higher severity and an

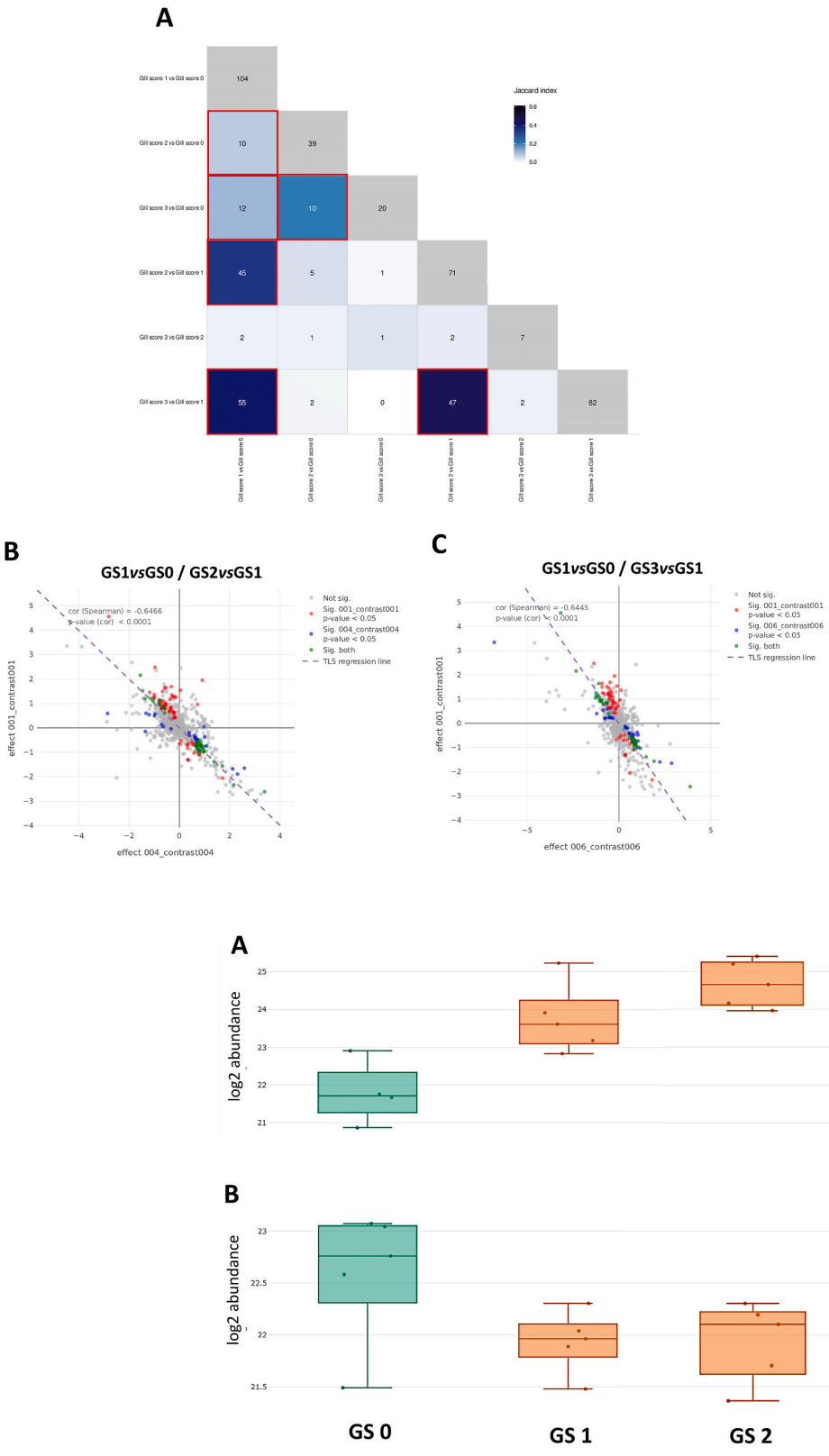

Fig. 3. A) Heatmap showing the number of overlapping selected metabolites between the contrasts performed. Note that the numbers on the diagonal represent the total number of selected metabolites found for each contrast. For each comparison, the value in the plot represents the number of intersecting selected metabolites, and the colour represents the Jaccard index (the intersection over the union) for the two types of contrast under consideration. The box with a red border indicates that the overlap is statistically significant (defined using p-value $<$ 0.05). **B–C**) Scatter plot comparing significant metabolites in **B)** GS1*vs*GS0 versus GS3*vs*GS1. Metabolites are represented by points and **C)** shows GS1*vs*GS0 versus GS2*vs*GS1. The colour of the point indicates which set the metabolite is assigned to. For each metabolite, the log2(fold change) in the GS1*vs*GS0 contrast (y-axis) and the log2(fold change) in the GS2*vs*GS1 **(B)**/GS3*vs*GS1 **(C)** contrast (x-axis) are shown.

Fig. 4. Plasma level (Log2 abundance) of **A)** adrenaline and **B)** adenosine in healthy and AGD-affected salmon. Both of these metabolites were found in all AGD-affected fish, and their level was significantly different from GS0 (p-value $<$ 0.05). Values given are from five individual fish.

impaired local inflammatory response [10]; whether this is related to the downregulation of circulating adenosine remains an open question. On the other hand, hypoxia is a possible consequence of compromised gill structures due to AGD. The production of adenosine under hypoxic condition is critical for adaptation, maintenance of cellular function, and protection of hypoxia-induced tissue injury [39]. Therefore, the reduced level of adenosine in infected fish suggests that this crucial mechanism had been likely inhibited, which could result in other

pathophysiological alterations if the infection progresses further.

Hippuric acid (Level 1 annotation) increased in response to infection showing a significant 3-fold increase in salmon with a GS1 compared to those with a gill score of 0 (Supplementary File 2). Similar trends were observed in GS2 compared to GS0. Hippuric acid is a metabolic derivative of benzoic acid, but its role in fish is still largely unknown [40]. In mammals, it is a biomarker for high dose exposure to certain toxic compounds such as toluene and is also commonly used as an indicator of renal health [41]. It remains to be explored whether such association is likewise present in salmon though the strikingly elevated levels in salmon with low AGD infection warrants further studies.

The tryptophan metabolite indole-3-lactic acid (ILA) decreased in response to the initial stage of infection with a significant 1.8-fold decrease in salmon with a GS1 compared to GS0. ILA abundance appears to return to baseline at the later stages of infection showing no significant reduction in salmon with GS2 or 3 compared to GS0. Note that the annotation level 2a was assigned to ILA in the data set indicating some uncertainty in the annotation of compound TF00162 as ILA.

We performed MetaCyc pathway analysis to identify pathways enriched in DAM. Enrichment analysis yielded significant results mainly when GS0 and GS1 were compared (Fig. 5A); the same comparison that showed the highest number of DAM (Fig. 2). Of the 208 compounds with annotation levels 2b or higher, only 101 were included in the MetaCyc database limiting the functional enrichment analysis. This also reflects

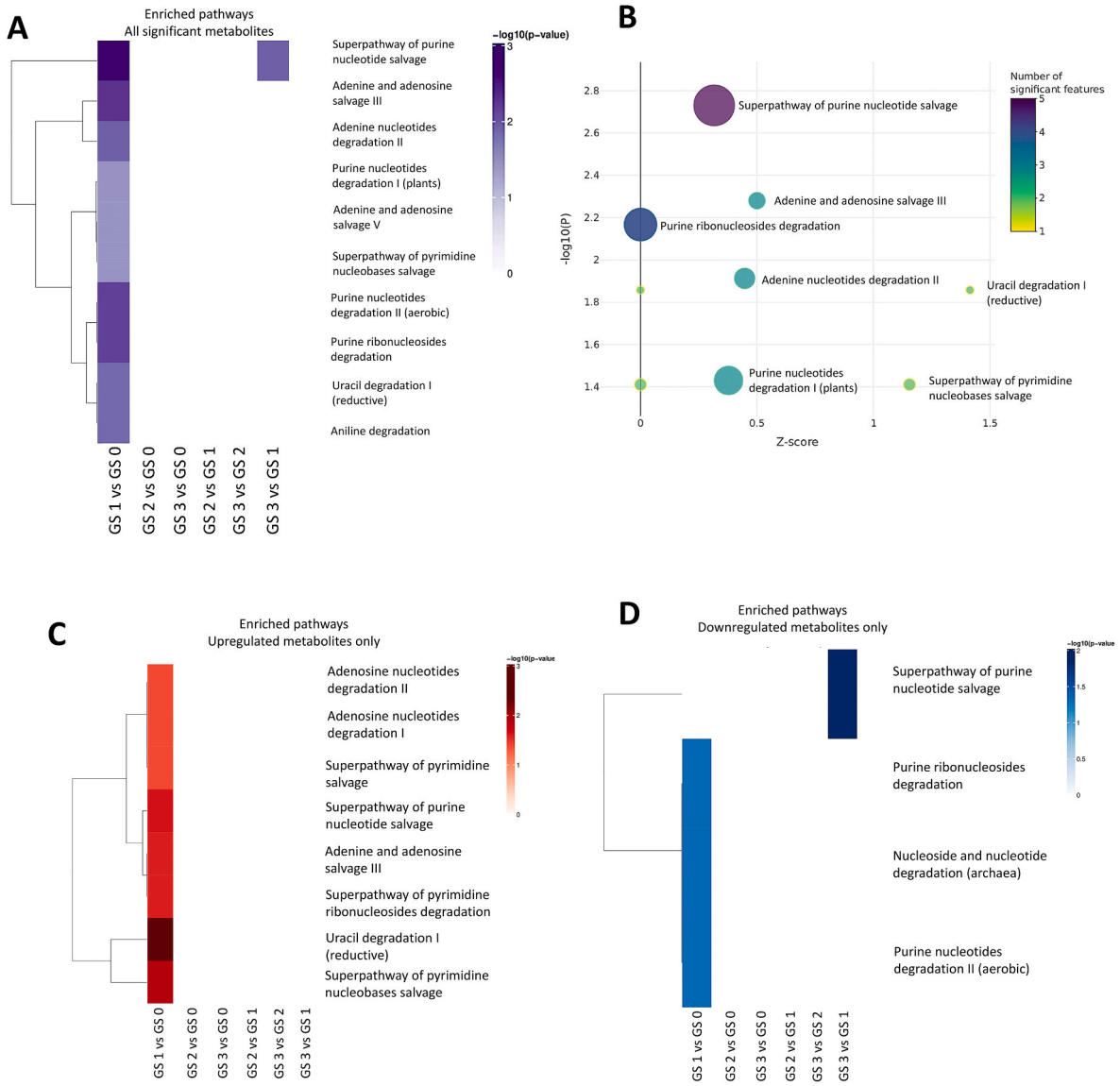

Fig. 5. Comparisons are shown on the X axis with MetaCyc pathways on the Y axis. When performing tests for enrichment, pathways were restricted to include only those with two or more compounds. Note that for the purposes of display, only MetaCyc pathways with enrichment p-values less than 0.05 were included. The results show the **(A)** union of significant up- and down-regulated metabolites as well as for significant **(C)** up-regulated and significant **(D)** down-regulated metabolites separately. Note that different compounds of a given MetaCyc pathway may be both up- and down-regulated within a single comparison. Red, blue, and purple indicate up-regulated, down-regulated, and the union of up- and down-regulated compounds, respectively. These colors were assigned based on the -log10 (enrichment p-value) with lighter colors implying less significant enrichment. Hierarchical clustering was applied to pathways (rows). The most significant pathways were clustered according to Euclidean distance using the complete linkage method. **(B)** Significant up- and down-regulated metabolites (at p-value < 0.05) in the GS1vsGS0 comparison were mapped to 16 compounds and assessed for MetaCyc pathway enrichment. The pathways reported were limited to those with two or more compounds. These significantly enriched pathways are indicated by purple boxes in the MetaCyc pathway heatmap in the overview section. Enrichment analyses with enrichment Z-score on the X axis and -log10(p-value) on the y-axis. Point size represents pathway size and point colour represents Z-score calculated as $Z=(Su-Sd)/N--\sqrt{Z=(Su-Sd)/N}$ where Su and Sd are the number of significant up-regulated and down-regulated compounds in the pathway, respectively, and N is the total number of compounds in the pathway.

the status of metabolomics in fish research, which is still in its infancy. There were ten enriched pathways (p-value<0.05) regardless of the direction of change (Fig. 5A). Most were represented by pathways with upregulated metabolites (Fig. 5C and D). Looking closer into the affected pathways in GS0*vs*GS1, the super pathway of purine nucleotide salvage showed the most well-represented DAM including adenosine, guanosine, hypoxanthine, inosine, and L-glutamate (Figs. 5B and 6). This was also the only pathway enriched in GS3*vs*GS1. Fig. 6 shows a reconstructed MetaCyc pathway of the purine nucleotide salvage super pathway showing key metabolites significantly affected by the early stage of AGD infection. The upregulation of metabolites associated with purine nucleotide salvage—especially inosine, hypoxanthine, and L-glutamate in the low infection level before returning to pre-infection levels in the later stages of infection—might indicate a role for the pathway in the early infection response. Nucleotide balance is critically important in maintaining cellular functions and integrity. In eukaryotes, this is maintained by *de novo* synthesis and salvage of nucleosides formed during degradation of RNA and DNA. Imbalance or deficiencies in nucleotide salvage and synthesis have been implicated in neurological disorders and DNA damage [42]. Previous studies have indicated that AGD may result in DNA damage either by differential modulation of growth arrest and DNA damage-inducible gene-45 beta gene [43] or

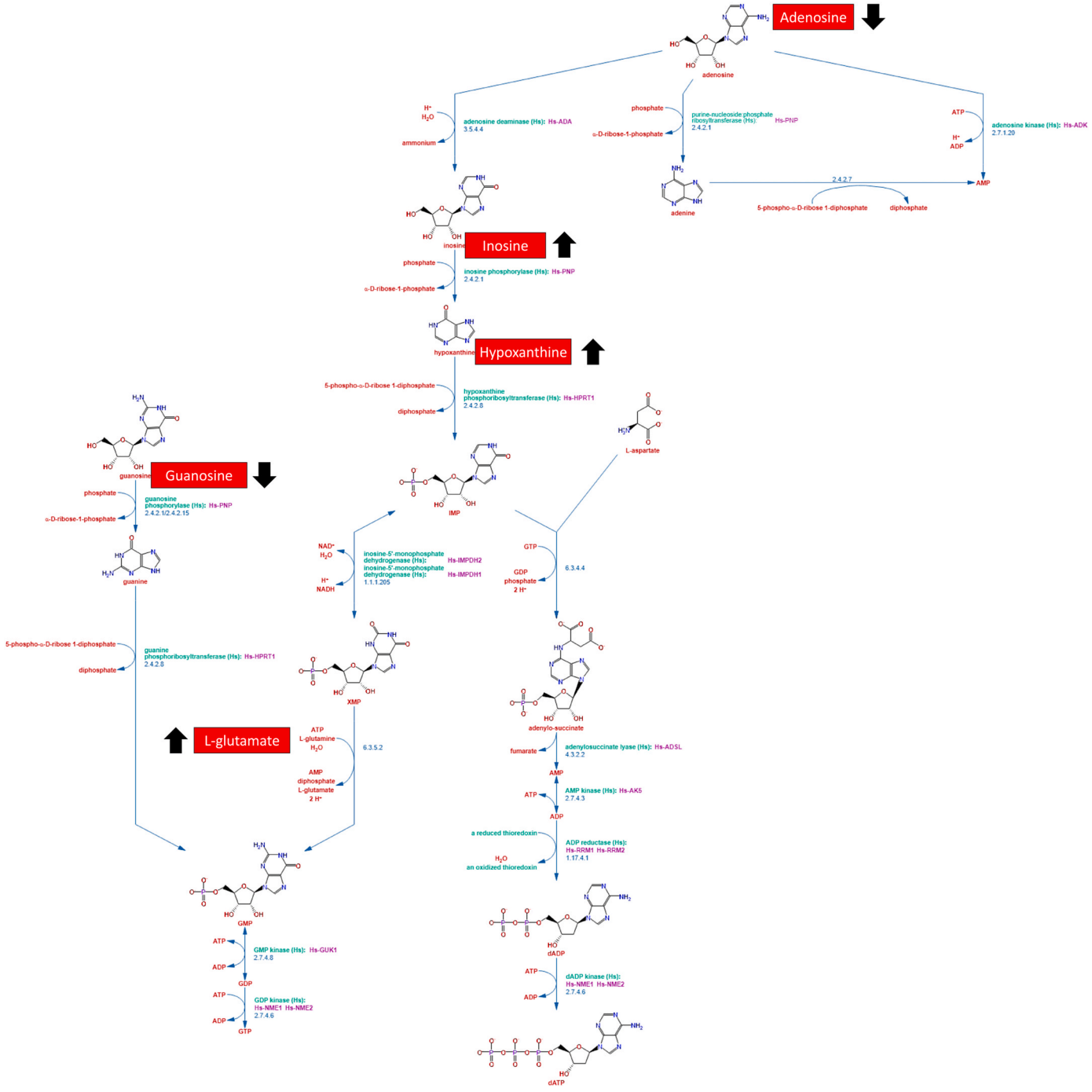

Fig. 6. MetaCyc superpathway of purine nucleotide salvage. Metabolites found to be significantly affected within the pathway are highlighted in red boxes. The upward/downward arrow indicates the direction of change in the comparison GS1*vs*GS0; such comparisons yielded a significant enrichment. The pathway diagram was generated from MetaCyc database [45].

oxidative damage through induction of oxidative stress [44]. It is likely that the substantial changes in this pathway in GS1 may provide a compensatory response to ensure that this physiological threat is mitigated. The superpathway role of purine nucleotide salvage in salmon remains to be functionally elucidated. This study provided insight into its role during a parasitic infestation.

In summary, the modifications in the circulating plasma metabolome revealed the systemic impacts of AGD in salmon. It offered insights into the molecules salmon mobilised as physiological countermeasures to infection pressure. The metabolomic changes were more evident in fish with lower GS, and the infection level was not severe. We speculate that such a profile is related to the extensive metabolomic interventions so as the infection will not progress and be severe. Further, the metabolites with neuroendocrine functions showing pronounced changes during infection are likely involved in cellular trafficking, especially in the host immune response, thus offering insight into the neuro-immune axis associated with AGD. One limitation of the present study was that the infected fish were taken from a common garden trial, thereby, the confounding impact of tank environment was not accounted. We acknowledge that the challenge concentration is higher than the concentration of amoebae in farm environment, which is often an issue in lab-based AGD trials. In addition, the farm environment is complex and there are issues that present as confounding factors to AGD. In particular, gill health-related issues such as complex gill disease, proliferative gill disease, proliferative gill inflammation, to name a few, are often detected together with AGD [46]. How these diseases/disorders affect the host metabolome remains to be unravelled, though we believe that they may have varying degrees of impacts, which may interfere with the AGD-related metabolomic dysregulation reported in this study. Therefore, further studies are needed to verify the suitability of the identified metabolomic signatures of infection under different laboratory and field AGD scenarios. Moreover, a temporal map of the plasma metabolome during disease development is necessary to provide another depth of understanding of how infection alters the salmon metabolome and link these changes to host immunity using a multi-platform response profiling.

CRediT authorship contribution statement

Carlo C. Lazado: Conceptualization, Data curation, Formal analysis, Funding acquisition, Investigation, Methodology, Project administration, Supervision, Validation, Visualization, Writing – original draft, Writing – review & editing. **Mette W. Breiland:** Conceptualization, Formal analysis, Investigation, Methodology, Resources, Writing – review & editing. **Francisco Furtado:** Formal analysis, Investigation, Methodology, Writing – review & editing. **Erik Burgerhout:** Conceptualization, Investigation, Methodology, Writing – review & editing. **David Strand:** Conceptualization, Formal analysis, Investigation, Methodology, Project administration, Resources, Software, Writing – review & editing.

Declaration of competing interest

The authors declare that they have no known competing financial interests or personal relationships that could have appeared to influence the work reported in this paper.

Data availability

Data will be made available on request.

Acknowledgements

The study received funding from the Norwegian Seafood Research Fund (ref. 901472) and the Norwegian Research Council (ref. 194050). We thank Sigurd Hytterød and Saima Nasrin Mohammad (NVI) for the amoeba culture, Mona Gjessing for the histology (NVI), Morten Marienborg (HiT) for the assistance in fish husbandry, Ragnhild Stenberg Berg and Gunhild Johansson (Nofima) for help with sample collection, Lea Johnsen (MS Omics ApS) for the metabolomic analysis, and Laura Bennet and Alexander Raeside (Fios Genomics) for the bioinformatics. F. F. wishes to acknowledge the ERASMUS+ Student Mobility Programme for financing his research stay at Nofima.

Appendix A. Supplementary data

Supplementary data to this article can be found online at https://doi.org/10.1016/j.micpath.2022.105553.

References

[1] T. Steinum, A. Kvellestad, L.B. Rønneberg, H. Nilsen, A. Asheim, K. Fjell, S.M. R. Nygård, A.B. Olsen, O.B. Dale, First cases of amoebic gill disease (AGD) in Norwegian seawater farmed Atlantic salmon, *Salmo salar* L., and phylogeny of the causative amoeba using 18S cDNA sequences, J. Fish. Dis. 31 (3) (2008) 205–214.
[2] N.D. Young, P.B.B. Crosbie, M.B. Adams, B.F. Nowak, R.N. Morrison, *Neoparamoeba perurans* n. sp., an agent of amoebic gill disease of Atlantic salmon (*Salmo salar*), Int. J. Parasitol. 37 (13) (2007) 1469–1481.
[3] M.B. Adams, B.F. Nowak, Distribution and structure of lesions in the gills of Atlantic salmon, *Salmo salar* L., affected with amoebic gill disease, J. Fish. Dis. 24 (9) (2001) 535–542.
[4] R.S. Taylor, W.J. Muller, M.T. Cook, P.D. Kube, N.G. Elliott, Gill observations in Atlantic salmon (*Salmo salar*, L.) during repeated amoebic gill disease (AGD) field exposure and survival challenge, Aquaculture 290 (1) (2009) 1–8.
[5] M.L. Kent, T.K. Sawyer, R.P. Hedrick, *Paramoeba pemaquidensis* (Sarcomastigophora: Paramoebidae) infestation of the gills of coho salmon *Oncorhynchus kisutch* reared in sea water, Dis. Aquat. Org. 5 (3) (1988) 163–169.
[6] T. Oldham, H. Rodger, B.F. Nowak, Incidence and distribution of amoebic gill disease (AGD) — an epidemiological review, Aquaculture 457 (2016) 35–42.
[7] R. Taylor, C. Huynh, D. Cameron, B. Evans, M. Cook, G. Ritchie, Gill Score Guide - Amoebic Gill Disease (AGD) Management Training Document, 2016.
[8] R.N. Morrison, P.B.B. Crosbie, B.F. Nowak, The induction of laboratory-based amoebic gill disease revisited, J. Fish. Dis. 27 (8) (2004) 445–449.
[9] N.D. Young, G.A. Cooper, B.F. Nowak, B.F. Koop, R.N. Morrison, Coordinated down-regulation of the antigen processing machinery in the gills of amoebic gill disease-affected Atlantic salmon (*Salmo salar* L.), Mol. Immunol. 45 (9) (2008) 2581–2597.
[10] M. Marcos-López, J.A. Calduch-Giner, L. Mirimin, E. MacCarthy, H.D. Rodger, I. O'Connor, A. Sitjà-Bobadilla, J. Pérez-Sánchez, M.C. Piazzon, Gene expression analysis of Atlantic salmon gills reveals mucin 5 and interleukin 4/13 as key molecules during amoebic gill disease, Sci. Rep. 8 (1) (2018) 13689.
[11] Y. Pennacchi, M.J. Leef, P.B.B. Crosbie, B.F. Nowak, A.R. Bridle, Evidence of immune and inflammatory processes in the gills of AGD-affected Atlantic salmon, Salmo salar L, Fish Shellfish Immunol. 36 (2) (2014) 563–570.
[12] V.A. Valdenegro-Vega, P. Crosbie, A. Bridle, M. Leef, R. Wilson, B.F. Nowak, Differentially expressed proteins in gill and skin mucus of Atlantic salmon (*Salmo salar*) affected by amoebic gill disease, Fish Shellfish Immunol. 40 (1) (2014) 69–77.
[13] M. Marcos-López, C. Espinosa Ruiz, H.D. Rodger, I. O'Connor, E. MacCarthy, M.Á. Esteban, Local and systemic humoral immune response in farmed Atlantic salmon (*Salmo salar* L.) under a natural amoebic gill disease outbreak, Fish Shellfish Immunol. 66 (2017) 207–216.
[14] M. McCormack, E. Dillon, I. O'Connor, E. MacCarthy, Investigation of the initial host response of naïve Atlantic salmon (*Salmo salar*) inoculated with Paramoeba perurans, Microorganisms 9 (4) (2021) 746.
[15] N.A. Botwright, A.R. Mohamed, J. Slinger, P.C. Lima, J.W. Wynne, Host-parasite interaction of Atlantic salmon (Salmo salar) and the Ectoparasite Neoparamoeba perurans in amoebic gill disease, Front. Immunol. 12 (1900) (2021).
[16] T. Young, A.C. Alfaro, Metabolomic strategies for aquaculture research: a primer, Rev. Aquacult. 10 (1) (2018) 26–56.
[17] R. Mayeux, Biomarkers: potential uses and limitations, NeuroRx 1 (2) (2004) 182–188.
[18] R. Lulijwa, A.C. Alfaro, T. Young, Metabolomics in salmonid aquaculture research: applications and future perspectives, Rev. Aquacult. (2022).
[19] C.E. Doneanu, W. Chen, J.R. Mazzeo, UPLC/MS monitoring of water-soluble vitamin Bs in cell culture media in minutes, Water Application Note 720004042en, 2011.
[20] C.C. Lazado, L.R. Sveen, M. Soleng, L.-F. Pedersen, G. Timmerhaus, Crowding reshapes the mucosal but not the systemic response repertoires of Atlantic salmon to peracetic acid, Aquaculture 531 (2021), 735830.
[21] M. Fernández-García, D. Rojo, F. Rey-Stolle, A. García, C. Barbas, Metabolomic-based methods in diagnosis and monitoring infection progression, Exp. Suppl. 109 (2018) 283–315.
[22] I. Barber, H.A. Wright, Effects of Parasites on Fish Behaviour: Interactions with Host Physiology, Fish Physiology, Academic Press, 2005, pp. 109–149.
[23] J. Maertzdorf, J. Weiner 3rd, S.H. Kaufmann, Enabling biomarkers for tuberculosis control, Int. J. Tubercul. Lung Dis. 16 (9) (2012) 1140–1148.

[24] C.F. Low, M.Z.H. Rozaini, N. Musa, B. Syarul Nataqain, Current knowledge of metabolomic approach in infectious fish disease studies, J. Fish. Dis. 40 (10) (2017) 1267–1277.
[25] D. Zilberg, B.L. Munday, Pathology of experimental amoebic gill disease in Atlantic salmon, *Salmo salar* L., and the effect of pre-maintenance of fish in sea water on the infection, J. Fish. Dis. 23 (6) (2000) 401–407.
[26] S. Haddeland, C.C. Lazado, G.V. Merkin, O.J. Myre, M.A. Okubamichael, L.-F. Pedersen, K. Pittman, Dynamic morphometrics of mucous cells reveal the minimal impact of therapeutic doses of peracetic acid on Atlantic salmon gill health, Aquaculture 534 (2021), 736315.
[27] M.J. Leef, J.O. Harris, M.D. Powell, Metabolic effects of amoebic gill disease (AGD) and chloramine-T exposure in seawater-acclimated Atlantic salmon *Salmo salar*, Dis. Aquat. Org. 78 (1) (2007) 37–44.
[28] O. Benedicenti, T.G. Pottinger, C. Collins, C.J. Secombes, Effects of temperature on amoebic gill disease development: does it play a role? J. Fish. Dis. 42 (9) (2019) 1241–1258.
[29] M. McCormack, E. Dillon, I. O'Connor, E. MacCarthy, Investigation of the initial host response of naïve Atlantic salmon (*Salmo salar*) inoculated with *Paramoeba perurans*, Microorganisms 9 (4) (2021).
[30] B. Everts, Metabolomics in immunology research, Methods Mol. Biol. 1730 (2018) 29–42.
[31] R. Flysand, J.A. Ask, G. Serck-Hanssen, K.B. Helle, Plasma catecholamines and accumulation of adrenaline in the atrial cardiac tissue of aquacultured Atlantic salmon (*Salmo salar*) during stress, J. Fish. Biol. 41 (1) (1992) 103–111.
[32] M. Hvas, E. Karlsbakk, S. Mæhle, D.W. Wright, F. Oppedal, The gill parasite *Paramoeba perurans* compromises aerobic scope, swimming capacity and ion balance in Atlantic salmon, Conserv. Physiol. 5 (1) (2017).
[33] Y. Cao, A.K. Tveten, A. Stene, Establishment of a non-invasive method for stress evaluation in farmed salmon based on direct fecal corticoid metabolites measurement, Fish Shellfish Immunol. 66 (2017) 317–324.
[34] T. Yada, T. Nakanishi, Interaction between endocrine and immune systems in fish, Int. Rev. Cytol. 220 (2002) 35–92.
[35] H. Guo, B. Dixon, Understanding acute stress-mediated immunity in teleost fish, Fish Shellfish Immunol. Rep. 2 (2021), 100010.
[36] A. Depelchin, J.J. Letesson, Adrenaline influence on the immune response. II. Its effects through action on the suppressor T-cells, Immunol. Lett. 3 (4) (1981) 207–213.
[37] C. Silva-Vilches, S. Ring, K. Mahnke, ATP and its metabolite adenosine as regulators of dendritic cell activity, Front. Immunol. 9 (2018) 2581.
[38] H. Kälvegren, J. Fridfeldt, T. Bengtsson, The role of plasma adenosine deaminase in chemoattractant-stimulated oxygen radical production in neutrophils, Eur. J. Cell Biol. 89 (6) (2010) 462–467.
[39] H. Liu, Y. Xia, Beneficial and detrimental role of adenosine signaling in diseases and therapy, J. Appl. Physiol. 119 (10) (2015) 1173–1182.
[40] M.O. James, J.B. Pritchard, In vivo and in vitro renal metabolism and excretion of benzoic acid by a marine teleost, the southern flounder, Drug Metab. Dispos. 15 (5) (1987) 665–670.
[41] H.J. Lees, J.R. Swann, I.D. Wilson, J.K. Nicholson, E. Holmes, Hippurate: the natural history of a mammalian-microbial cometabolite, J. Proteome Res. 12 (4) (2013) 1527–1546.
[42] M. Fasullo, L. Endres, Nucleotide salvage deficiencies, DNA damage and neurodegeneration, Int. J. Mol. Sci. 16 (5) (2015) 9431–9449.
[43] R.N. Morrison, G.A. Cooper, B.F. Koop, M.L. Rise, A.R. Bridle, M.B. Adams, B. F. Nowak, Transcriptome profiling the gills of amoebic gill disease (AGD)-affected Atlantic salmon (*Salmo salar* L.): a role for tumor suppressor p53 in AGD pathogenesis? Physiol. Genom. 26 (1) (2006) 15–34.
[44] J.W. Wynne, M.G. O'Sullivan, M.T. Cook, G. Stone, B.F. Nowak, D.R. Lovell, N. G. Elliott, Transcriptome analyses of amoebic gill disease-affected Atlantic salmon (*Salmo salar*) tissues reveal localized host gene suppression, Mar. Biotechnol. 10 (4) (2008) 388–403.
[45] R. Caspi, R. Billington, C.A. Fulcher, I.M. Keseler, A. Kothari, M. Krummenacker, M. Latendresse, P.E. Midford, Q. Ong, W.K. Ong, S. Paley, P. Subhraveti, P.D. Karp, The MetaCyc database of metabolic pathways and enzymes, Nucleic Acids Res. 46 (D1) (2017) D633–D639.
[46] A.S. Boerlage, A. Ashby, A. Herrero, A. Reeves, G.J. Gunn, H.D. Rodger, Epidemiology of marine gill diseases in Atlantic salmon (*Salmo salar*) aquaculture: a review, Rev. Aquacult. 12 (4) (2020) 2140–2159.